Inorg. Chem. **2004**, *43*, 3998–4006

Inorganic Chemistry
Article

Synthesis and Structure of Alkaline Earth Silicon Nitrides: $BaSiN_2$, $SrSiN_2$, and $CaSiN_2$

Zoltán A. Gál, Phillip M. Mallinson, Heston J. Orchard, and Simon J. Clarke*

Inorganic Chemistry Laboratory, Department of Chemistry, University of Oxford,
South Parks Road, Oxford OX1 3QR, U.K.

Received January 26, 2004

The alkaline earth silicon nitrides $AESiN_2$ (AE = Ca, Sr, Ba) are reported, synthesized as clear, colorless, single crystals from molten sodium at 900–1100 °C or, in the cases of $BaSiN_2$ and $SrSiN_2$, as white powders by reacting powdered intermetallics AESi with flowing anhydrous ammonia at 550–1000 °C. Structures were determined from single-crystal X-ray diffraction measurements at 150 K: $BaSiN_2$ crystallizes in space group *Cmca* (No. 64) with $a = 5.6046(1)$ Å, $b = 11.3605(3)$ Å, $c = 7.5851(2)$ Å, and $Z = 8$. The structure consists of pairs of SiN_4 tetrahedra edge-linked to form bow-tie-shaped Si_2N_6 dimers which share vertexes to form layers and has no analogue in oxide chemistry. $SrSiN_2$ has a distorted form of this structure ($SrSiN_2$: space group $P2_1/c$ (No. 14), $a = 5.9750(5)$ Å, $b = 7.2826(7)$ Å, $c = 5.4969(4)$ Å, $\beta = 113.496(4)°$, $Z = 4$). The structure of $CaSiN_2$ contains only vertex-sharing SiN_4 tetrahedra, linked to form a three-dimensional stuffed-cristobalite type framework isostructural with $KGaO_2$ ($CaSiN_2$: space group *Pbca* (No. 61), $a = 5.1229(3)$ Å, $b = 10.2074(6)$ Å, $c = 14.8233(9)$ Å, $Z = 16$).

Introduction

There is an increasing interest in non-oxide solids, and some nitrides and nitride-containing compounds have important electronic or structural properties complementary to those of oxides. Silicon nitride, Si_3N_4, is an important ceramic material,[1,2] and there exist also a wide range of ternary nitridosilicates containing a formally anionic $SiN_x^{(3x-4)-}$ framework and electropositive countercations. Many of these materials have been synthesized in the group of Schnick and co-workers[3] by the reaction between alkaline earth metals and/or lanthanides with silicon diimide at elevated temperatures (e.g. >1500 °C) achieved using a radio frequency induction furnace. In general, silicon adopts tetrahedral coordination in nitrides with the only known exceptions of the recently discovered high-pressure phase c-Si_3N_4,[4] with the spinel structure and both SiN_4 tetrahedra and SiN_6 octahedra, and the oxide nitride $Ce_{16}Si_{15}O_6N_{32}$.[5] However, there are important differences between nitridosilicates and the familiar oxosilicate analogues. First, while the Si−O frameworks in oxosilicates contain terminal Si−O bonds or Si−O−Si linkages at the common vertexes of two SiO_4 tetrahedra, nitrogen exhibits a greater range of coordinations by silicon in nitridosilicates. Nitrogen is often found to have three Si neighbors ($N^{[3]}$); these can appear together with $N^{[2]}$ atoms, for example in $AE_2Si_5N_8$,[6,7] or even with $N^{[4]}$ atoms in $BaYbSi_4N_7$.[8] Terminal Si−N bonds ($N^{[1]}$) are found in $Ba_5Si_2N_6$,[9] Recent calculations on such compounds have shown that the $N^{[n]}$ 2p-derived crystal orbitals which dominate the top of the valence band decrease in energy as n increases in a series of nitridosilicates ($1 \leq n \leq 4$).[10] Second, the nitride anion is more polarizable than the oxide anion and one consequence of this is that edge-sharing of SiN_4 tetrahedra is not forbidden in nitridosilicates, as it is in oxosilicates, since the ensuing Si−Si repulsion is screened

---

* Author to whom correspondence should be addressed. E-mail: simon.clarke@chem.ox.ac.uk. Fax: +44 1865 272690. Tel: +44 1865 272600.

(1) Petzow, G.; Herrmann, M. *Struct. Bonding* **2002**, *102*, 47.
(2) Rosenflanz, A. *Curr. Opin. Solid State Mater. Sci.* **1999**, *4*, 453.
(3) Schnick, W.; Huppertz, H.; Lauterbach, R. *J. Mater. Chem.* **1999**, *9*, 289.
(4) Soignard, E.; Somayazulu, M.; Dong, J. J.; Sankey, O. F.; McMillan, P. F. *J. Phys.: Condens. Matter* **2001**, *13*, 557.
(5) Kollisch, K.; Schnick, W. *Angew. Chem., Int. Ed.* **1999**, *38*, 357.
(6) Schlieper, T.; Schnick, W. *Z. Anorg. Allg. Chem.* **1995**, *621*, 1037.
(7) Schlieper, T.; Milius, W.; Schnick, W. *Z. Anorg. Allg. Chem.* **1995**, *621*, 1380.
(8) Schnick, W.; Huppertz, H. *Angew. Chem., Int. Ed. Engl.* **1996**, *35*, 1983.
(9) Yamane, H.; DiSalvo, F. J. *J. Alloys Compd.* **1996**, *240*, 33.
(10) Fang, C. M.; Hintzen, H. T.; de With, G.; de Groot, R. A. *J. Phys.: Condens. Matter* **2001**, *13*, 67. Fang, C. M.; Li, Y. Q.; Hintzen, H. T.; de With, G. *J. Mater. Chem.* **2003**, *13*, 1480.

10.1021/ic049901p CCC: $27.50

by the induced dipoles on the polarizable bridging anions.[11] (There is only one unconfirmed report of edge sharing of SiO_4 tetrahedra in a polymorph of SiO_2.[12]) Edge sharing of SiN_4 tetrahedra has been observed both in the silicon-rich $BaSi_7N_{10}$,[13] synthesized by Schnick and co-workers at 1650 °C, and in the barium-rich $Ba_5Si_2N_6$,[9] synthesized by Yamane and DiSalvo at 750 °C in molten sodium, in which isolated $Si_2N_6^{10-}$ anions are composed of a pair of edge-sharing SiN_4 tetrahedra. Edge sharing of MN_4 tetrahedra has also been reported in several alkaline earth gallium and aluminum nitrides, including the isostructural pairs $AE_3Ga_2N_4$ (AE = Sr,[14] Ba[15]) and $AE_3Al_2N_3$ (AE = Sr,[16] Ba[17]) and $Ca_3Ga_2N_4$,[14] which contrast with the vertex-sharing only of GaO_4 tetrahedra in gallates. $Li_4Sr_3Ge_2N_6$[18] contains a $[Ge_2N_6]^{10-}$ anion composed of a pair of edge-sharing GeN_4 tetrahedra. In addition to the $BaSi_7N_{10}$[13] and $Ba_5Si_2N_6$[9] stoichiometries described above, several other alkaline earth nitridosilicates are known, including the structurally related series $AE_2Si_5N_8$ (AE = Ca,[6] Sr, Ba[7]) with exclusively vertex-sharing SiN_4 tetrahedra and the compounds $AESiN_2$ (AE = Be,[19] Mg,[20,21] Ca,[22] Sr,[23] Ba[24]) which have been reported but for which only the ordered wurtzite structures of $BeSiN_2$ and $MgSiN_2$ with three-dimensional frameworks of vertex-sharing SiN_4 tetrahedra are known. $BaSiN_2$ has been reported synthesized as a powder by solid-state reaction between binary barium and silicon nitrides,[24] but although a tentative orthorhombic unit cell was obtained by indexing the powder diffraction pattern, no suitable structural model could be deduced by comparison with isostoichiometric oxides. As part of a program investigating low-temperature approaches to ternary nitride synthesis by reacting intermetallic compounds with ammonia, which has received only very limited attention in the past,[25] we have synthesized bulk crystalline $BaSiN_2$ at much lower temperatures (550 °C) than previously used. Although we were unable to deduce a structural model on the basis of the information available from the powder diffraction pattern, we have determined the crystal structure of this compound by the analysis of single crystals grown from molten sodium at 900−1100 °C. Powder and single-crystal samples of $SrSiN_2$ and single crystals of $CaSiN_2$ have also been obtained enabling comparison of the structures of $AESiN_2$ for all alkaline earths and comparison with the structures of isostoichiometric oxides, chalcogenides, and pnictides.

Table 1. Contents of the Tantalum Tubes for Reactions Used to Synthesize Crystals of the Compounds $AESiN_2$ (AE = Ca, Sr, Ba)[a]

compd	reacn temp/°C	NaN_3/mg	AE/mg	Si/mg	Na/mg
$BaSiN_2$	1100	63	206	21	200
$SrSiN_2$	1000	46	96	30	200
$CaSiN_2$	1000	70	33	46	200

[a] The amount of NaN_3 was chosen to give a maximum possible pressure inside the tube of 35 atm; the tantalum tubes used were of different volumes.

Experimental Section

Synthesis. Most of the reactants and products used in this work are air-sensitive, so all manipulations of solids were carried out in a Glovebox Technology argon-filled recirculating drybox with a combined O_2 and H_2O content of less than 5 ppm. For the synthesis of single crystals, alkaline earth metal pieces (Ba, 99+%, Aldrich; Sr, 99%, Aldrich; Ca, 99.5%, ALFA), silicon (99.9999%, Alfa Aesar, finely ground in the drybox), sodium azide (99%, Aldrich), and sodium (99+%, BDH) were placed in a tantalum tube (9 mm outer diameter, 0.5 mm wall thickness, 120 mm long) which was sealed under 1 atm of purified argon and then sealed inside an evacuated silica ampule. The amount of NaN_3 used in each case was adjusted to keep the maximum possible nitrogen pressure constant at 35 atm for all temperatures, and approximately 200 mg of Na was added as a “flux”. For reactions carried out at 1100 °C with a Ba:Si molar ratio of 2:1, which were found to produce the largest yield of high-quality crystals, the contents of the tantalum tube were as follows: NaN_3, 63 mg; Ba, 206 mg; Si, 21 mg; Na, 200 mg. The tubes were heated in a chamber furnace at 3 °C min^{-1} to temperatures of 900 or 1100 °C, soaked at these temperatures for 48 h, and then cooled at 0.1 °C min^{-1} to 400 °C whence the furnace was switched off. The sodium was removed by sublimation under dynamic vacuum at 350 °C. Single crystals were extracted by dispersing the product in Paratone oil. The syntheses of crystals of $SrSiN_2$ and $CaSiN_2$ were carried out at 1000 °C, and the contents of the tantalum tubes were as summarized in Table 1.

High yields of the target phases were obtained in these reactions, although the crystals produced were often small and of poor quality. While the elements were found to be suitable starting materials for the syntheses carried out in molten sodium, binary alkaline earth nitrides can also be used as sources of the metals and of some of the nitrogen in the products. Sr_2N[26] was prepared on the 1.5 g scale by the reaction between freshly cut Sr pieces and flowing nitrogen gas (Air Products, oxygen free, and additionally cleaned by flowing over a Ti wire “getter” held at 800 °C) at 900 °C for 48 h. Stoichiometric amounts (i.e. Sr:Si = 1:1) of Sr_2N (189.3 mg) and Si (56 mg) were sealed in a tantalum tube with 150 mg of Na and 22 mg of NaN_3, and the tube was heated at 1100 °C. The product was pure white $SrSiN_2$ (powder and small crystals) according to laboratory powder X-ray diffraction (PXRD) measurements, and this sample was used for powder neutron diffraction (PND) measurements. Additionally, $BaSiN_2$ and $SrSiN_2$ were synthesized as bulk powders by reacting the intermetallics BaSi or SrSi with ammonia. BaSi was synthesized from stoichiometric amounts of the elements by reacting 2.49 g of barium lump (99+%, Aldrich, and with the oxide coating removed by filing) with 0.5093 g of silicon powder (99.9999%, Alfa Aesar) in a 9 mm diameter tantalum tube which was sealed under 1 atm of argon to avoid evaporation

---

(11) Madden, P. A.; Wilson, M. *Chem. Soc. Rev.* **1996**, 339.
(12) Weiss, A.; Weiss, A. *Z. Anorg. Allg. Chem.* **1954**, *276*, 95.
(13) Huppertz, H.; Schnick, W. *Chem.*−*Eur. J.* **1997**, *3*, 249.
(14) Clarke, S. J.; DiSalvo, F. J. *Inorg. Chem.* **1997**, *36*, 1143.
(15) Yamane, H.; DiSalvo, F. J. *Acta Crystallogr., Sect C: Cryst. Struct. Commun.* **1996**, *52*, 760.
(16) Blase, W.; Cordier, G.; Ludwig, M.; Kriep, R. *Z. Naturforsch., B* **1994**, *49*, 501.
(17) Ludwig, M.; Niewa, R.; Kniep, R. *Z. Naturforsch, B* **1999**, *54*, 461.
(18) Park, D. G.; Gál, Z. A.; DiSalvo, F. J. *J. Solid State Chem.* **2003**, *172*, 166.
(19) Rabenau, A.; Eckerlin, P. *Naturwissenschaften* **1959**, *46*, 106.
(20) David, J.; Laurent, Y.; Lang, J. *Bull. Soc. Fr. Mineral. Cristallogr.* **1970**, *93*, 153.
(21) Bruls, R. J.; Hintzen, H. T.; Metselaar, R.; Loong, C.-K. *J. Phys. Chem. Solids* **2000**, *61*, 1285.
(22) Laurent, Y.; Lang, J. *C. R. Acad. Sci. Paris* **1966**, *262*, 103.
(23) Gaudé, J.; Lang, J. *C. R. Acad. Sci. Paris* **1969**, *268*, 1785.
(24) Morgan, P. E. D. *J. Mater. Sci. Lett.* **1984**, *3*, 131.
(25) Guyader, J.; Maunaye, M.; Lang, J. *C. R. Acad. Sci. Paris* **1971**, *272*, 311.
(26) Brese N. E.; O’Keeffe M. *J. Solid State Chem.* **1990**, *87*, 134.

of barium.[27] The tantalum tube was protected inside an evacuated silica jacket and heated at 900 °C for 48 h. BaSi does not melt congruently, and the sample was therefore annealed at 825 °C for 25 days. The gray product was confirmed to be BaSi using laboratory PXRD. SrSi was synthesized in a similar way by reacting 2.9444 g of strontium pieces (99%, Aldrich) with 0.9438 g of silicon powder in a sealed tantalum tube at 1200 °C for 4 days, followed by annealing at 1130 °C for 30 days.

To form $BaSiN_2$, 1.8 g of finely ground BaSi was spread along the length of a 4 cm long alumina boat which was placed in a 22 mm internal diameter silica tube. The tube was placed inside a split tube furnace and purged with ammonia (NH_3, 99.98%, BOC, and cleaned further by storage over sodium). The temperature was raised to 550 °C at a rate of 7 °C min^{-1} and maintained at this temperature under a flow of ammonia of approximately 3 dm^3 h^{-1} for a period of 24 h whence the flow tube was isolated from the ammonia flow and removed from the furnace allowing the sample to cool to room temperature. The tube was evacuated and returned to the drybox; the white product was ground and then heated at 900 °C under flowing ammonia for a further 24 h to improve the crystallinity. The reaction of SrSi with ammonia was accomplished in a similar way: SrSi was heated in anhydrous ammonia for periods of 24 h at 600, 800, and 1000 °C with intermediate regrinding in the drybox. In this case heating at 1000 °C was required to obtain a white, fully oxidized, product.

Chemical Analysis. Energy-dispersive analysis of X-rays (EDX) was carried out on single crystals using a JEOL JSM-840A scanning electron microscope equipped with an Oxford Instruments ISIS300 energy-dispersive X-ray analysis system. It was not possible to obtain quantitative analysis for nitrogen using this instrument. Combustion analysis for nitrogen on bulk powders was carried out using a Carlo Erber Strumentazione 1106 CHN analyzer.

X-ray Powder Diffraction. Some measurements were made using a Siemens D5000 diffractometer operating in Debye–Scherrer geometry with Cu $K\alpha_1$ radiation selected using a Ge(111) monochromator. The samples were ground with amorphous boron (1:1 mass ratio) to limit sample absorption and sealed in 1 mm diameter glass capillaries. Alternatively, measurements were made using a Phillips PW 1729/10 diffractometer operating in Bragg–Brentano geometry with Cu $K\alpha_1/\alpha_2$ radiation and equipped with a diffracted beam monochromator. Samples were contained within an airtight sealed holder.

Single-Crystal X-ray Diffraction. Crystals protected under Paratone oil were mounted in a nylon loop and immobilized in the frozen oil at 150 K using an Oxford Instruments cooling system integral to the single-crystal diffractometer. High-redundancy data sets were collected down to 0.7 Å resolution using an Enraf-Nonius FR590 κCCD diffractometer using Mo $K\alpha$ radiation ($\lambda = 0.710\ 71$ Å) achieved using a graphite monochromator. Data were analyzed with the DENZO-SMN programs.[28] Heavy atoms were located using direct methods, after which nitrogen atoms were located from difference Fourier maps. Analytical absorption corrections[29] were carried out in the cases of $BaSiN_2$ and $SrSiN_2$, and the structure refinements were completed using SHELXL-97.[30]

Neutron Powder Diffraction. Time-of-flight powder neutron diffraction (PND) data were collected using the diffractometer POLARIS at the ISIS Facility, Rutherford Appleton Laboratory. Measurements were made on $BaSiN_2$ derived from the nitridation of BaSi at 900 °C and on a sample of $SrSiN_2$ obtained using the sodium flux route at 1100 °C. Diffraction patterns were measured in the d-spacing range $0.5 < d < 8$ Å by means of three banks of detectors located at scattering angles 2θ of 35° (^{3}He tube detector), 90° (ZnS scintillator), and 145° (^{3}He tube detector, highest resolution bank: $\Delta d/d = 5 \times 10^{-3}$) for a total integrated proton current at the production target of 380 μA h for 2.0 g of $BaSiN_2$ and 1445 μA h for 0.25 g of $SrSiN_2$ at room temperature. The samples were contained in cylindrical thin-walled vanadium cans sealed under 1 atm of Ar with indium gaskets. Data for $BaSiN_2$ at 4 K (372 μA h) were obtained in an “ILL orange” cryostat. PND, and where appropriate PXRD, data were analyzed using the Rietveld profile refinement suite GSAS.[31] Refinement against data collected on POLARIS was carried out using all three detector banks simultaneously.

Table 2. Results of Single-Crystal X-ray and Neutron Refinements (at 298 and 4 K) of $BaSiN_2$

		powder	
parameter	single crystal at 150 K	298 K	4 K
formula	$BaSiN_2$	$BaSiN_2$	$BaSiN_2$
radiation	Mo $K\alpha$, $\lambda = 0.710\ 73$ Å	Neutron	Neutron
instrument	Enraf-Nonius FR590 κCCD	POLARIS	POLARIS
space group	*Cmca*	*Cmca*	*Cmca*
fw	193.43	193.43	193.43
a/Å	5.6046(1)	5.60430(5)	5.6009(2)
b/Å	11.3605(3)	11.3655(1)	11.3490(4)
c/Å	7.5851(2)	7.59965(7)	7.5844(3)
V/Å^3	482.95(2)	484.06(1)	482.11(5)
Z	8	8	8
ρ_{calc}/Mg m^{-3}	5.321	5.309(1)	5.330(1)
no. of variables	25	89	86
R1	0.0138		
wR2	0.0282		
χ^2		1.110	0.885
wR$_p$		0.0115	0.0074
R$_{F^2}$		0.0197	0.0223

Results

$BaSiN_2$. Clear/colorless crystals of $BaSiN_2$ were isolated from reactions in molten sodium with a Ba:Si ratio of 2:1 at 900 and 1100 °C. EDX data produced a Ba:Si ratio of 0.53(3):0.47(3), and laboratory PXRD showed that $BaSiN_2$ was the majority phase in both reactions. The analysis of single-crystal data showed that higher quality crystals (mosaic spread of 0.7–1.0 °) were obtained in the reactions at 1100 °C compared with those obtained in reactions at 900 °C (mosaic spread of 1.5–1.7°). Structure solution by direct methods and subsequent refinement yielded a model in space group *Cmca* with $a = 5.6046(1)$ Å, $b = 11.3605(3)$ Å, $c = 7.5851(2)$ Å, and $Z = 8$, largely confirming Morgan’s proposal.[24] The refinement results are shown in Table 2, and the atomic positions and equivalent isotropic displacement parameters are listed in Table 3.

The mass change during the nitridation of BaSi by ammonia at 550 °C was consistent with full oxidation to form $BaSiN_2$:

$$BaSi + 2NH_3 \rightarrow BaSiN_2 + 3H_2$$

---

(27) Merlo, F.; Fornasini, M. L. *J. Less Common Met.* **1967**, *13*, 603.

(28) Nonius, Collect, Denzo, Scalepack, Sortav: *Kappa CCD Program Package*; Nonius BV: Delft, The Netherlands, 1998.

(29) Alcock, N. *Cryst. Comput.* **1970**, 271.

(30) Sheldrick, G. *A Program for Crystal Structure Determination*, release 97-2; University of Gottingen: Gottingen, Germany, 1997.

(31) Larson, A.; von Dreele, R. B. *The General Structure Analysis System*; Los Alamos National Laboratory: Los Alamos, NM, 1985.

Table 3. Atomic Parameters for $BaSiN_2$ Obtained from Single-Crystal X-ray Diffraction Data at 150 K and Powder Neutron Diffraction Data at 298 and 4 K[a]

atom	site	x	y	z	$100U_{iso,eq}$/Å^2
			Single-Crystal X-ray Diffraction		
Ba	8f	0	0.335 56(1)	0.065 23(2)	0.450(7)
Si	8f	0	0.049 41(6)	0.140 45(9)	0.29(1)
N1	8f	0	0.398 1(2)	0.419 2(3)	0.44(4)
N2	8e	0.25	0.097 8(2)	0.25	0.59(4)
			Powder Neutron Diffraction		
Ba	8f	0	0.335 82(4)	0.0651 3(6)	0.49(1)
			[0.335 72(4)]	[0.065 24(6)]	[0.056(6)]
Si	8f	0	0.049 38(4)	0.140 03(8)	0.29(1)
			[0.049 46(5)]	[0.139 91(9)]	[0.18(2)]
N1	8f	0	0.398 10(2)	0.419 97(3)	0.60(1)
			[0.398 04(3)]	[0.419 34(4)]	[0.38(1)]
N2	8e	0.25	0.097 15(2)	0.25	0.79(1)
			[0.097 95(3)]		[0.46(1)]

[a] Values in brackets are obtained from refinement against neutron powder diffraction data at 4 K.

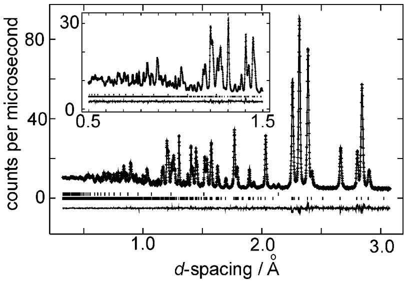

Figure 1. Results of Rietveld refinement of the structure of $BaSiN_2$ at 298 K against POLARIS data (145° detector bank). The measured (points), calculated, (line) and difference (lower line) profiles are shown. Tick marks indicate allowed reflections for the $BaSiN_2$ phase (lower set) and the vanadium sample container (upper set). The inset shows a magnification of the low *d*-spacing region.

Table 4. Results for Structure Refinements of $SrSiN_2$ against Single-Crystal X-ray and Powder Neutron Diffraction Measurements

parameter	single crystal	powder
formula	$SrSiN_2$	$SrSiN_2$
radiation	Mo Kα, $\lambda = 0.710\,73$ Å	neutrons
instrument	Enraf-Nonius FR590 κCCD	POLARIS
T/K	150(2)	298
space group	$P2_1/c$	$P2_1/c$
fw	143.73	143.73
a/Å	5.9750(5)	5.98139(6)
b/Å	7.2826(7)	7.32121(7)
c/Å	5.4969(4)	5.50425(6)
β/deg	113.496(4)	113.518(1)
V/Å^3	219.36(3)	221.014(5)
Z	4	4
ρ_{calc}/Mg m^{-3}	4.352	4.319
R1	0.0458	
wR2	0.0893	
χ^2		1.832
wR_p		0.0115
R_{F^2}		0.0275

Table 5. Refined Atomic Parameters for $SrSiN_2$

atom	site	x	y	z	$100U_{iso,eq}$/Å^2
			Single-Crystal X-ray Diffraction at 150 K		
Sr	4e	0.339 3(1)	0.5724(1)	0.175 6(1)	1.06(3)
Si	4e	0.107 7(4)	0.1419(3)	0.0671(4)	1.00(4)
N1	4e	0.210(1)	0.5905(8)	0.585(1)	1.0(1)
N2	4e	0.219(1)	0.2252(8)	0.385(1)	1.2(1)
			Powder Neutron Diffraction at 298 K		
Sr	4e	0.338 76(9)	0.573 82(8)	0.175 5(1)	0.83(3)
Si	4e	0.104 9(2)	0.141 9(1)	0.068 2(2)	0.33(4)
N1	4e	0.208 29(8)	0.587 73(6)	0.584 06(9)	0.73(2)
N2	4e	0.215 43(9)	0.224 39(6)	0.386 2(1)	0.89(2)

Combustion analysis of the white powder yielded 13.5(2)% by mass nitrogen, corresponding to a stoichiometry of $BaSiN_{1.87(3)}$. The powder diffraction pattern closely resembled that reported previously[24] and that obtained by PXRD analysis of the samples obtained from molten sodium. The material obtained after further reaction with ammonia at 900 °C was more crystalline (Bragg peaks 80% of the width of those of the sample prepared at 550 °C) and was used in further structural analysis. Refinement against PND data collected at 298 K and at 4 K, using as a starting model that obtained from the results of single-crystal analysis, proceeded without incident confirming the single-crystal result. The refinement results are presented in Table 2, and the fit at 298 K is shown in Figure 1. The atomic parameters at 298 and 4 K are compared with those of the single-crystal solution at 150 K in Table 3.

$SrSiN_2$. Extremely air-sensitive clear/colorless crystals were extracted from the gray powder obtained by the reaction between strontium and silicon (Sr:Si = 1:1) under nitrogen in molten sodium at 1000 °C (Table 1). EDX analysis indicated a Sr:Si ratio of 0.6:0.4, but this analysis was hampered by overlap between the main Sr and Si lines using this technique. The crystals were extremely thin with a needlelike habit and had a high mosaic spread (2°) resulting in noisy data. However, structure solution by direct methods and subsequent refinement confirmed that the stoichiometry was $SrSiN_2$ and yielded a model in the monoclinic space group $P2_1/c$ (No. 14) with $a = 5.9750(5)$ Å, $b = 7.2826(7)$ Å, $c = 5.4969(4)$ Å, $\beta = 113.496(4)°$, and $Z = 4$. The PXRD pattern of the sample which yielded these crystals of $SrSiN_2$ closely resembled that reported previously for an incompletely characterized sample of $SrSiN_2$.[23] Indeed this route is a convenient one for the synthesis of bulk $SrSiN_2$, and a sample prepared using a modification of this route with Sr_2N as the source of Sr (see above) at 1100 °C was the one used in the PND measurement. This measurement confirmed the monoclinic model and ruled out an alternative, but lower probability, orthorhombic cell. The refinement results from single-crystal X-ray and PND analysis are shown in Table 4, and the atomic positions and equivalent isotropic displacement parameters are listed in Table 5. The results of the refinement against PND data are shown in Figure 2. The formation of bulk $SrSiN_2$ by the reaction of SrSi with anhydrous ammonia is more difficult than in the case of $BaSiN_2$: while the reaction with BaSi is complete at 550 °C, and heating at 900 °C merely improves crystallinity, the mass gain indicating full conversion to white $SrSiN_2$ was only accomplished after reactions at 1000 °C. Furthermore, while the full widths at half-maximum of the Bragg peaks of the samples of $BaSiN_2$ and $SrSiN_2$ used in the PND investigations were similar (approximately 0.25° measured using the Philips laboratory X-ray diffractometer), the bulk sample of $SrSiN_2$ prepared at 1000 °C from the reaction of SrSi with ammonia had Bragg peaks 40% broader than those of the sample used in the PND measurement. Comparative

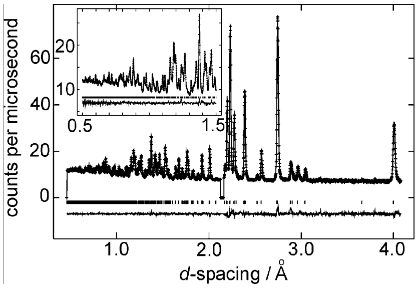

Figure 2. Results of Rietveld refinement of the structure of $SrSiN_2$ at 298 K against POLARIS data (90° detector bank). The measured (points), calculated (line), and difference (lower line) profiles are shown. Tick marks indicate allowed reflections for $SrSiN_2$. A reflection at 2.14 Å due to the vanadium sample container has been excluded from the refinement. The inset shows a magnification of the low *d*-spacing region.

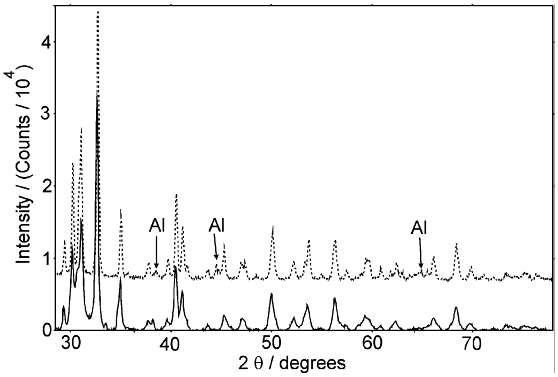

Figure 3. X-ray diffractograms (Cu $K\alpha_1/\alpha_2$ radiation) for the sample of $SrSiN_2$ prepared using the sodium flux method at 1100 °C and used in the PND measurements (top, dotted), and a sample prepared by the reaction between SrSi and flowing ammonia at 1000 °C (bottom, solid). The dotted line has been offset along the intensity axis for clarity, and peaks arising from the aluminum sample holder are marked.

Table 6. Results of Single-Crystal X-ray Refinement of $CaSiN_2$

formula	$CaSiN_2$
radiation	Mo Kα, $\lambda = 0.710\,73$ Å
instrument	Enraf-Nonius FR590 κCCD
physical form	single cryst
T/K	150
space group	*Pbca*
fw	96.19
a/Å	5.1229(3)
b/Å	10.2074(6)
c/Å	14.8233(9)
V/Å^3	775.13(8)
Z	16
ρ_{calc}/Mg m^{-3}	3.297
R1	0.0406
wR2	0.0818

laboratory powder X-ray diffractograms shown in Figure 3 confirm that nitridation by ammonolysis is viable for the formation of bulk $SrSiN_2$.

$CaSiN_2$. Clear/colorless platelets obtained from a reaction in molten sodium with Ca:Si ratio 1:2 were found to have a Ca:Si ratio of 0.516(5):0.484(5) by EDX. The crystals were often twinned and with a high mosaicity (2°), but a satisfactory solution was determined by direct methods and subsequent refinement. $CaSiN_2$: space group *Pbca* (No. 61), $a = 5.1229(3)$ Å, $b = 10.2074(6)$ Å, $c = 14.8233(9)$ Å, $Z = 16$. The refinement results are shown in Table 6, and the atomic positions and equivalent isotropic displacement parameters are listed in Table 7. The simulated PXRD pattern closely resembles that reported for material of composition $CaSiN_2$.[22]

Table 7. Refined Atomic Parameters for $CaSiN_2$ Determined at 150 K

atom	site	x	y	z	$100U_{iso,eq}$/Å^2
Ca1	8c	0.2414 (1)	0.009 68(7)	0.065 00(4)	1.19(2)
Ca2	8c	0.3462(1)	0.274 08(7)	0.187 59(4)	1.15(2)
Si1	8c	0.2265(2)	0.016 63(9)	0.312 08(6)	0.84(2)
Si2	8c	0.3172(2)	0.270 03(9)	0.437 22(6)	0.89(2)
N1	8c	0.0949(6)	0.477 4(3)	0.215 5(2)	1.13(6)
N2	8c	0.1495(6)	0.276 1(3)	0.035 4(2)	1.25(7)
N3	8c	0.1972(5)	0.426 8(3)	0.409 0(2)	1.11(6)
N4	8c	0.2762(6)	0.179 8(3)	0.338 2(2)	1.27(6)

Discussion

Structures of $BaSiN_2$ and $SrSiN_2$. The results of the structural analysis of $BaSiN_2$ indicate a new structure type unlike that of any isostoichiometric oxide or nitride analogues, as suggested by the results of Morgan.[24] A search of the ICSD and MDF databases revealed no matches for the Pearson symbol of oC32 and Wyckoff sequence f^3e for any compounds of this stoichiometry. The structure is shown in Figure 4: pairs of SiN_4 tetrahedra share edges to form "bow-tie" units Si_2N_6, previously identified in $Ba_5Si_2N_6$[9] and $BaSi_7N_{10}$.[13] In $BaSiN_2$ these units condense by vertex sharing of the four remaining unshared vertexes to form puckered two-dimensional sheets separated by barium ions. The analysis of PND data confirmed the full occupancy of the anion site by nitride and showed that the structure is unchanged on cooling to 4 K. The structure of $SrSiN_2$ is closely related to that of $BaSiN_2$, and the two structures are compared in Figures 4 and 5. Selected bond lengths and angles for $BaSiN_2$, determined from both single-crystal X-ray and PND data, are listed in Table 8, and the corresponding values determined for $SrSiN_2$ are listed in Table 9.

The detailed diagram of the Si_2N_6 unit of $BaSiN_2$ in Figure 4 shows that while the N2−Si−N2 angle of 109.18(8)° (Table 8) is close to the ideal tetrahedral angle, the N1−Si−N1 angle associated with the shared edge is greatly reduced to 94.8(1)°. Furthermore, the Si−N1 distances of 1.781(2) and 1.777(2) Å are substantially longer than the two Si−N2 distances of 1.7191(8) Å. These are consequences of repulsion between Si atoms separated by the shared tetrahedral edge, and these angles and the differences between the mean Si−N("bridging") and Si−N("terminal") distances in the Si_2N_6 units of $BaSi_7N_{10}$[13] and $Ba_5Si_2N_6$[9] are fairly similar. In $Ba_2Si_5N_8$,[7] with only corner-sharing SiN_4 tetrahedra, and including some cases of three tetrahedra sharing a common vertex ($N^{[3]}$), there is a wide range of Si−N distances (1.666−1.797 Å), but the N−Si−N angles are all in the range 103−115°. While the corresponding bond lengths and angles of $SrSiN_2$ (Figure 4, Table 9) are similar to those of $BaSiN_2$, Figure 5 shows that the effect of decreasing the size of the alkaline earth cation from Ba^{2+} to Sr^{2+} is distortion of the sheets of corner-linked Si_2N_6 units, by rotation about the linkages between Si_2N_6 units and lowering of the symmetry. In α-$Ca_3Ga_2N_4$,[14] also depicted in Figure 5, the $[GaN_2]^{3-}$ polyanion has the same topology

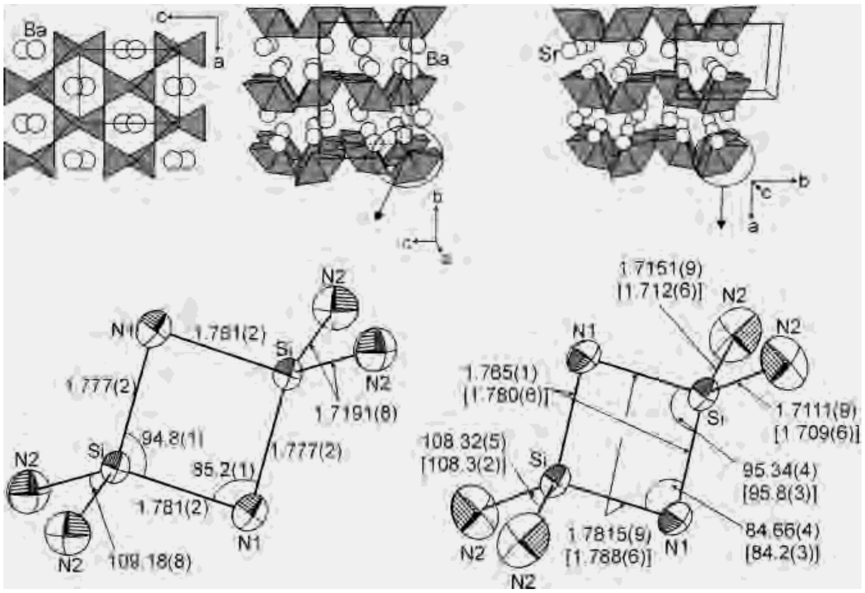

Figure 4. Crystal structures of $BaSiN_2$ (top: left and center) and $SrSiN_2$ (top: right) showing Si_2N_6 edge-sharing units linked at their remaining vertexes to form layers. In the detailed views of the Si_2N_6 unit in $BaSiN_2$ (bottom: left), bond lengths (in Å) and angles (in deg) and 99% displacement ellipsoids are shown determined from single-crystal X-ray measurements at 150 K. For $SrSiN_2$ (bottom: right), 99% displacement ellipsoids are derived from the refinement against PND data at 298 K along with corresponding bond distances (in Å) and angles (in deg); bond distances obtained from refinement against single-crystal X-ray data are in brackets. Full lists of comparative bond lengths and angles are given in Tables 8 and 9. A view of $SrSiN_2$ perpendicular to the layers appears in Figure 5.

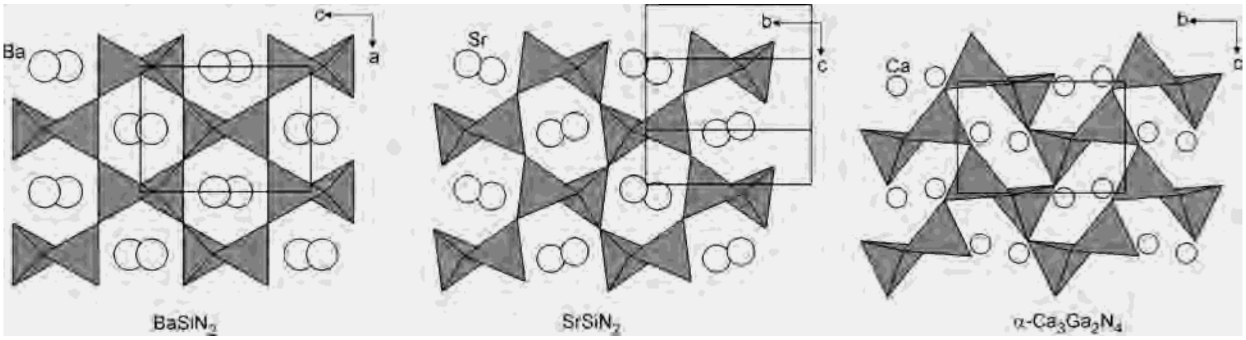

Figure 5. Comparison of the similar two-dimensional frameworks composed of pairs of edge-sharing tetrahedra joined at their remaining vertexes to form puckered two-dimensional layers. The structure is flexible, and the figure shows the effect of increasing the size of the alkaline earth cations accommodated in and between the layers in a series of main group ternary nitrides. The structure of α-$Ca_3Ga_2N_4$ is described in ref 14.

Table 8. Selected Bond Lengths (Å) and Angles (deg) for $BaSiN_2$[a]

bond length/angle	single crystal 150 K	neutron 298 K	neutron 4 K
Si−N1	1.781(2)	1.7778(6)	1.7763(6)
Si−N1	1.777(2)	1.7758(7)	1.7759(8)
Si−N2 [2]	1.7191(8)	1.7190(3)	1.7207(4)
Ba−N1 [2]	2.8935(6)	2.8923(2)	2.8907(2)
Ba−N1	2.877(2)	2.8805(6)	2.8745(6)
Ba−N1	2.777(2)	2.7851(5)	2.7772(5)
Ba−N2 [2]	2.8730(6)	2.8800(4)	2.8712(4)
Ba−N2 [2]	3.350(2)	3.3615(5)	3.3475(5)
Si−Si	2.408(1)	2.406(1)	2.401(1)
N2−Si−N2	109.18(8)	109.19(3)	108.93(4)
N1−Si−N1	94.8(1)	94.79(3)	94.95(3)
N2−Si−N1 [2]	115.60(8)	115.42(2)	115.61(3)
N2−Si−N1 [2]	110.40(6)	110.61(2)	110.48(3)
Si−N1−Si	85.2(1)	85.20(2)	85.05(3)
Si−N2−Si	142.7(2)	143.19(3)	142.69(4)

[a] The numbers in brackets indicate the number of bonds or angles of a particular type.

Table 9. Selected Bond Lengths (Å) and Angles (deg) for $SrSiN_2$

bond length/angle	single crystal 150 K	$SrSiN_2$ neutron 298 K
Si−N1	1.788(6)	1.7815(9)
Si−N1	1.780(6)	1.765(1)
Si−N2	1.709(6)	1.7111(9)
Si−N2	1.712(6)	1.7151(9)
Sr−N1	2.564(6)	2.5862(6)
Sr−N1	2.658(6)	2.6600(7)
Sr−N1	2.753(6)	2.7620(7)
Sr−N1	3.027(6)	3.0317(7)
Sr−N2	2.618(6)	2.6286(7)
Sr−N2	2.980(6)	3.0193(7)
Sr−N2	3.001(6)	3.0273(8)
Sr−N2	3.145(6)	3.1588(7)
Si−Si	2.391(4)	2.388(2)
N2−Si−N2	108.3(2)	108.32(5)
N1−Si−N1	95.8(3)	95.34(4)
N2−Si−N1	115.8(3)	115.80(5)
N2−Si−N1	117.5(3)	117.89(6)
N2−Si−N1	111.4(3)	111.14(5)
N2−Si−N1	107.1(3)	107.30(5)
Si−N1−Si	84.2(3)	84.66(4)
Si−N2−Si	135.6(4)	135.82(6)

as the $[SiN_2]^{2-}$ polyanion in $BaSiN_2$ and $SrSiN_2$ but is distorted to an even greater degree than that in $SrSiN_2$.

The distortions are presumably driven by the coordination requirements of the electropositive cations. In $BaSiN_2$, Ba is coordinated by six nitrogen atoms at distances of between 2.77 and 2.90 Å and two further ions are located at 3.350(2)

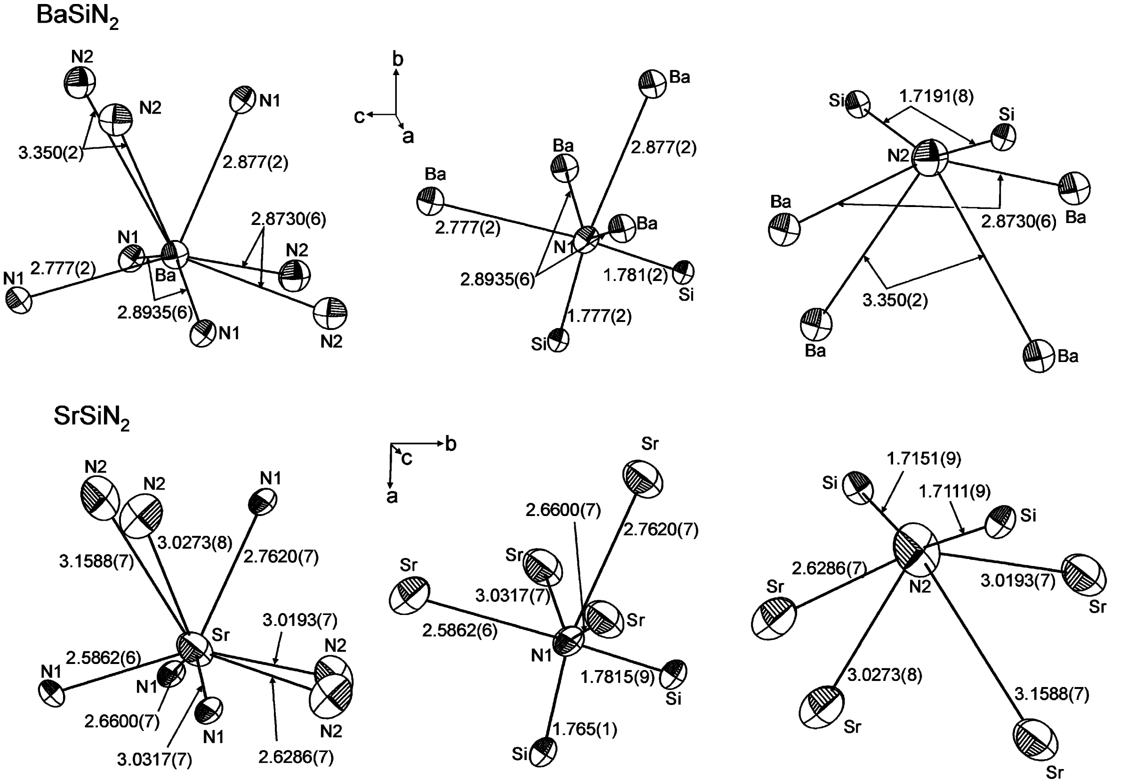

Figure 6. Comparative coordination geometries around the barium, strontium, and nitrogen atoms in $BaSiN_2$ (above) and $SrSiN_2$ (below). Displacement ellipsoids are shown at the 99% level, and the diagrams have the same orientations with respect to the crystallographic axes as the corresponding structure diagrams in Figure 4. The displacement ellipsoids and bond lengths (in Å) for $BaSiN_2$ are from the single-crystal X-ray refinement at 150 K. For $SrSiN_2$, the corresponding parameters are derived from the refinement against PND data at 298 K, because the single crystal was of a relatively poor quality. Full lists of the bond lengths derived from different measurements are given in Tables 8 and 9.

Å as shown in Figure 6. In $SrSiN_2$, only four nitride ions are located between 2.55 and 2.77 Å from Sr, and there are four other nitride ions at long bonding distances of between 2.97 and 3.13 Å. Both nitrogen atoms in $BaSiN_2$ are coordinated by two Si atoms and four Ba atoms in highly distorted octahedral arrangements as shown in Figure 6. N2, which links two adjacent Si_2N_6 units by their vertexes, is more strongly bonded to Si than N1, which links two SiN_4 tetrahedra at an edge to form the Si_2N_6 units. Correspondingly, the mean Ba−N1 distance of 2.86 Å is shorter than the mean Ba−N2 distance of 3.11 Å. The coordinations of the nitrogen atoms in $SrSiN_2$ (Figure 6) are geometrically similar to those in $BaSiN_2$, although with lower symmetry as a consequence of the distortion on decreasing the size of the alkaline earth cation.

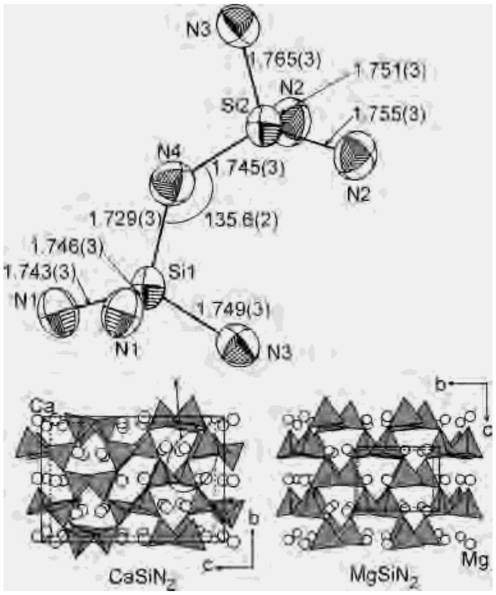

Figure 7. Cristobalite-derived structure of $CaSiN_2$ compared with the wurtzite-derived structure of $MgSiN_2$.[21] Displacement ellipsoids for the detail of the SiN_4 tetrahedra of $CaSiN_2$ determined at 150 K from X-ray single-crystal data are shown at the 99% level. A full list of bond lengths and angles is given in Table 10.

Structure of $CaSiN_2$. $CaSiN_2$, like the analogous compounds of the lighter alkaline earths, contains SiN_4 tetrahedra which are joined only at their vertexes. The structure of $CaSiN_2$ is shown in Figure 7, and bond lengths and angles are listed in Table 10. Crystals of $CaSiN_2$ have recently been prepared independently by Ottinger and Nesper,[32] who have determined the same structure as that reported here. This structure is evidently more stable under the experimental conditions employed for $CaSiN_2$ synthesis than the $BaSiN_2$-type structure with a framework more heavily distorted than in $SrSiN_2$, such as that found in α-$Ca_3Ga_2N_4$[14] (Figure 5). The arrangement of vertex-linked tetrahedra in $CaSiN_2$ is the D1-type tilting distortion of the idealized C9-type β-cristobalite framework.[33] If the alkaline earth cation is

---

[32] Ottinger, F.; Nesper, R. *Acta Crystallogr., Sect. A: Foundations of Crystallography* **2002**, *58* (Supplement), C337.

[33] Thompson, J. G.; Withers, R. L.; Palethorpe, S. R.; Melnitchenko, A. *J. Solid State Chem.* **1998**, *141*, 29.

Table 10. Selected Bond Lengths (Å) and Angles (deg) for $CaSiN_2$

Si1−N4	1.729(3)	Ca1−N1	2.406(3)	Ca1−N2	2.794(3)
Si1−N1	1.743(3)	Ca1−N3	2.412(3)	Ca1−N3	3.022(3)
Si1−N1	1.746(3)	Ca1−N3	2.431(3)		
Si1−N3	1.749(3)	Ca1−N2	2.488(3)		
Si2−N4	1.745(3)	Ca2−N4	2.434(3)	Ca2−N3	2.778(3)
Si2−N2	1.751(3)	Ca2−N4	2.458(3)	Ca2−N1	2.827(3)
Si2−N2	1.755(3)	Ca2−N2	2.470(3)		
Si2−N3	1.765(3)	Ca2−N1	2.477(3)		
N4−Si1−N1	109.1(1)	N4−Si2−N2	109.3(2)	Si1−N1−Si1	129.4(2)
N4−Si1−N1	114.4(1)	N4−Si2−N2	119.8(2)	Si2−N2−Si2	131.2(2)
N1−Si1−N1	104.5(1)	N2−Si2−N2	107.07(9)	Si1−N3−Si2	126.3(2)
N4−Si1−N3	106.7(1)	N4−Si2−N3	103.7(1)	Si1−N4−Si2	135.6(2)
N1−Si1−N3	115.9(1)	N2−Si2−N3	111.2(1)		
N1−Si1−N3	106.4(1)	N2−Si2−N3	105.6(1)		

smaller than Ca^{2+}, the structure adopted is based on a different arrangement of vertex-linked tetrahedra, and $MgSiN_2$[20,21] and $BeSiN_2$[19] have a cation-ordered wurtzite-type structure. Indeed the same relationship exists in the alkali metal gallates: $MgSiN_2$ and $BeSiN_2$ are isostructural with one polymorph of $NaGaO_2$,[34] while $CaSiN_2$ is isostructural with $KGaO_2$.[34] Although the relationship between the structures of $MgSiN_2$ and $CaSiN_2$ is not a simple one, Figure 7 compares the two structures showing that the orientation of the SiN_4 tetrahedra in $MgSiN_2$ results in a noncentrosymmetric structure, as found for the wurtzite archetype. $CaGeN_2$ has been reported[35] with the B1-type (β-$KCoO_2$) tilting distortion of the β-cristobalite structure. All the nitrogen atoms in $CaSiN_2$ are at the shared vertexes of a pair of vertex-shared tetrahedra. The mean of the Si−N distances in $CaSiN_2$ (Table 10) is 1.748(9) Å; this is similar to the mean values in $BaSiN_2$ (1.75(3) Å) and $SrSiN_2$ (1.75(4) Å), although in these compounds in which there is some edge-sharing of SiN_4 tetrahedra, and consequently two types of Si−N bond, as discussed above, the standard deviations in the values are much larger. Ca1 is surrounded by four N atoms located between 2.40 and 2.49 Å (i.e. at distances similar to the sum of the ionic radii[36]) and by two further N atoms which complete an approximately octahedral geometry. Ca2 is in a highly distorted octahedral environment, again with four shorter Ca−N distances (between 2.43 and 2.48 Å) and two longer distances of around 2.8 Å. Since all the SiN_4 tetrahedra share all their vertexes, all the nitrogen atoms are coordinated to two Si atoms. All the N atoms are also coordinated by two further Ca atoms located 2.40−2.49 Å distant. N1 and N2 are coordinated by a further Ca atom each at around 2.8 Å to give distorted five-coordinate geometries. N3 is coordinated by two further Ca atoms at 2.777(3) and 3.023(3) Å and might be considered six-coordinate, while N4 is probably best considered four-coordinate in a distorted tetrahedral environment. Distances are listed in Table 10.

Comparison with Other Compounds. The structure of $BaSiN_2$ is one that has no known analogue in oxide chemistry and which, like many other nitridosilicates, contains edge-shared SiN_4 tetrahedra. These are not found in the analogous oxides because this would entail too much repulsion of the tetrahedral atom across the shared edge. All the members of the *AE*SiN_2 (*AE* = Be, Mg, Ca, Sr, Ba) family contain nitrogen atoms exclusively coordinated by two silicon atoms ($N^{[2]}$), but while $BaSiN_2$ and $SrSiN_2$ have a framework containing both edge- and vertex-sharing SiN_4 tetrahedra, the isostoichiometric compounds of the smaller alkaline earths adopt structures in which the $[SiN_2]^{2-}$ anionic framework is exclusively constructed from vertex-sharing tetrahedra. This trend for the larger alkaline earths to favor condensation of the tetrahedra at their edges is also found in other nitrides: $Ba_3Ga_2N_4$[15] and $Sr_3Ga_2N_4$[14] contain infinite chains of GaN_4 tetrahedra each sharing a pair of opposing edges, while α-$Ca_3Ga_2N_4$,[14] with a framework similar to that in $BaSiN_2$, has both edge- and vertex-sharing, (but β-$Ca_3Ga_2N_4$[37] is constructed from GaN_4 tetrahedra which share only vertexes). The condensation of SiN_4 tetrahedra by edge sharing is presumably driven by the coordination requirements of the larger alkaline earth cations and is possible because nitride is sufficiently polarizable to accommodate the close approach of silicon atoms.[11] Edge-sharing of tetrahedra in main group compounds containing the more polarizable heavier chalcogenides and pnictides is common: $Ca_3Al_2As_4$[38] is isostructural with α-$Ca_3Ga_2N_4$,[14] with a framework similar to that in $BaSiN_2$ and $SrSiN_2$, but we have been unable to identify any compounds isostructural with $BaSiN_2$ or $SrSiN_2$. $KGaS_2$[39] contains a double layer of all-vertex-linked GaS_4 tetrahedra, while, with the larger Cs^+ ion, the GaS_4 tetrahedra share a pair of opposite edges with two neighboring tetrahedra, as in $Sr_3Ga_2N_4$[14] and $Ba_3Ga_2N_4$,[15] to form infinite chains in $CsGaS_2$[40] (the structure of Rb analogue has not been reported). $LaCuS_2$[41] matches the space group, Pearson symbol (mP16), and Wyckoff sequence (e^4) of $SrSiN_2$ but is not isostructural because although it does contain layers composed of Cu_2S_6 units comprising a pair of edge-sharing CuS_4 tetrahedra, in this case the S atoms participating in edge-sharing are coordinated by a further Cu atom in a neighboring unit producing $S^{[3]}$ and some S atoms are coordinated by only one Cu atom ($S^{[1]}$). $TaCoTe_2$ and $NbCoTe_2$[42] contain layers of edge- and vertex-sharing $CoTe_4$ tetrahedra forming layers similar to those in $BaSiN_2$ and $SrSiN_2$ and with Co−Co bonds across the shared tetrahedral edges. However, in these cases the group 5 metal occupies 5-coordinate sites within the layers, and these are truly layered compounds. In $NaAuSe_2$,[43] the $[AuSe_2]^-$ framework is the direct analogue of the framework in $BaSiN_2$ and $SrSiN_2$ but with SiN_4 tetrahedra replaced by $AuSe_4$ square planar units as expected for Au^{III}.

Conclusions. We have shown that the oxidative nitridation of intermetallics using ammonia is a convenient route for

---

(34) Müller, H.-P.; Hoppe, R. *Z. Anorg. Allg. Chem.* **1992**, *611*, 73.

(35) Maunaye, M.; Guyader, J.; Laurent, Y.; Lang, J. *Bull. Soc. Fr. Mineral. Cristallogr.* **1971**, *94*, 347.

(36) Shannon, R. D. *Acta Crystallogr.* **1976**, *A32*, 751.

(37) Clarke, S. J.; DiSalvo, F. J. *J. Alloys Compd.* **1998**, *274*, 118.

(38) Cordier, G.; Czech, E.; Jakowski, M.; Schäfer, H. *Rev. Chim. Miner.* **1981**, *18*, 9.

(39) Lemoine, P.; Carre, D.; Guittard, M. *Acta Crystallogr.* **1984**, *C40*, 910.

(40) Schmitz, D.; Bronger, W. *Z. Naturforsch., B* **1975**, *30*, 491.

(41) Julien-Pouzol, M.; Jaulmes, S.; Mazurier, A.; Guittard, M. *Acta Crystallogr.* **1981**, *B37*, 1901.

(42) Li, J.; McCulley, F.; McDonnell, S. L.; Masiocchi, N.; Proserpio, D. M.; Sironi, A. *Inorg. Chem.* **1993**, *32*, 4829.

(43) Park, Y.; Kanatzidis, M. G. *J. Alloys Compd.* **1997**, *257*, 137.

the synthesis of bulk ternary nitrides, which in the case of $BaSiN_2$, for example, may be employed at relatively low temperatures. We are currently investigating the wide use of this route in the synthesis of novel nitrides. The structures of $BaSiN_2$ and $SrSiN_2$ appear to have no direct analogues in oxide chemistry or in the chemistry of the heavier chalcogenides or pnictides.

Acknowledgment. We are grateful to the U.K. Engineering and Physical Sciences Research Council for funding under Grant GR/R53296. S.J.C. acknowledges the further research support of the Royal Society. We thank Dr. N. Charnley (Department of Earth Sciences, University of Oxford) for assistance with the EDX analysis and Dr. R. I. Smith (ISIS facility) for assistance with the neutron diffraction investigations.

Supporting Information Available: X-ray crystallographic data in CIF format. This material is available free of charge via the Internet at http://pubs.acs.org.

IC049901P